RESEARCH PAPER

CrossMark

An improved bulk acoustic waves chip based on a PDMS bonding layer for high-efficient particle enrichment

Xi Shu[1] · Huiqin Liu[1] · Yezi Zhu[1] · Bo Cai[1] · Yanxia Jin[2] · Yongchang Wei[2] · Fuling Zhou[2] · Wei Liu[1] · Shishang Guo[1]

Abstract
In this work, we developed a feasible way to package bulk acoustic waves chip with sandwich structure by inserting a polydimethylsiloxane (PDMS) layer as the adhesive between cover glass and silicon substrate. After spin-coating and curing process, a PDMS layer was formed on one side of the cover glass and then bonded to the silicon substrate with microchannels by oxygen plasma treating. Both simulation and experiment showed that the chip was not leaking and the acoustic waves produced by the piezoelectric transducer could be propagated through the PDMS layer. Finally, a standing wave field was formed in the microchannels. Compared with traditional chip bonded by anodic bonding, simulation results showed that this packaging method did decrease the acoustic pressure in the channel, but the reduction was acceptable. After optimizing the experimental parameters, we successfully aggregated 15-μm silica spheres under a very low input power (21 dBm) at a flow velocity of 1 ml/h, and the enrichment efficiency of silica spheres was greater than 97%.

1 Introduction

Aggregation, manipulation and separation of cells and particles of microscale are very important in microfluidic system, and some methods were generally adopt such as electrophoresis (Dittrich et al. 2006; Li et al. 2007), magnetophoresis (Inglis et al. 2004; Yu et al. 2013), optical-based (Hoi et al. 2009; Wang et al. 2005) and acoustic-based methods (Petersson et al. 2007; Shi et al. 2009b). Among these methods, acoustic-based methods are popular because of their safe, label-free and contactless nature, so we focus on acoustic-based methods.

Acoustic-based methods are particle manipulation means based on acoustic waves, and they can be divided into two categories: surface acoustic waves (SAWs) and bulk acoustic waves (BAWs) according to the different acoustic wave modes (Lenshof et al. 2012a). The former mainly propagates in the surface of objects. Through SAWs generated by interdigital transducers on LiNbO$_3$ substrate, Tony et al. have achieved precise 3D manipulation of particles and very good cell sorting purity (Ding et al. 2012; Guo et al. 2016; Li et al. 2015; Ren et al. 2015). Unlike SAWs, the latter propagates in the interior of objects. Through the BAWs chip, Laurell et al. can achieve very high throughput in cell sorting (Antfolk et al. 2015b; Grenvall et al. 2015; Jakobsson et al. 2015). Compared with SAWs chip, BAWs chip attracted much attention owing to its high throughput in clinical application.

In BAWs chip, the acoustic waves are produced by vibration of piezoelectric transducer (PZT), and particles move to the pressure nodes or antinodes in the standing wave field formed by the two column of the same acoustic waves (Hawkes et al. 2002; Nilsson et al. 2004). The forces acting on the particle in the field depend on special physical characteristics of particles themselves such as size, density, compressibility, without any label. At present, the general method for BAWs chip packaging is anodic bonding (Antfolk et al. 2015a; Urbansky et al. 2016), however, which is complicated and these operations must be completed in the experimental environment with high temperature, high

✉ Fuling Zhou
zhoufuling@whu.edu.cn

✉ Shishang Guo
gssyhx@whu.edu.cn

1   Key Laboratory of Artificial Micro- and Nano-structures of Ministry of Education, School of Physics and Technology, Wuhan University, Wuhan 430072, China

2   Department of Hematology, Zhongnan Hospital of Wuhan University, Wuhan 430071, China

pressure and high voltage (Shields et al. 2016). According to Shields's work, the anodic bonding process was completed under a high temperature of 450 °C and a high voltage of 1000 V; meanwhile, the operators were exposed to the experimental environment. Therefore, the experimental environment was dangerous to the operators. In addition, the cost for anodic bonding machine and hard borosilicate cover glass is also very expensive. Besides anodic bonding, some other methods have also been applied to package BAWs chip; for example, someone packaged the chip with a glass lid by pressure of clamps; however, the BAWs chip is proved not totally sealed.

Therefore, we demonstrate a simple, safe and cheap method for chip packaging, which can be completed at room temperature, and the bonding equipment is oxygen plasma cleaner common in micromachining Laboratory, and the cover glass used for chip packaging is only ordinary laboratory glass slides. Through the enrichment of 15-μm silica spheres, we confirmed that our packaging method is practical and stable.

2 Experiment

2.1 Silicon channel fabrication

The device was fabricated on a 500 μm in thickness <100>-oriented silicon wafer, which was covered with silicon dioxide layer with a thickness of 1 μm on both sides. The channel structures were patterned by standard photolithography on one side the silicon wafer with AZ-5214E photoresist. Then, the silicon wafer was etched in 5%HF solution, while a layer of solidified polydimethylsiloxane (PDMS) (RTV615, GE Toshiba, USA) protected the backside because the silicon dioxide layer on the backside was needed in the next step. After etching and removing the PDMS layer and photoresist, the silicon wafer was anisotropic wet-etched in KOH solution (50 g/100 ml H_2O, 85 °C) for 85 min, performed with agitation by a magnetic stirrer at 400 rpm. The main channel structures were oriented 45° in relation to the primary flat of the wafer with a depth of 150 μm and a width of 375 μm. At last, the wafer was cut into pieces (60 mm × 20 mm) by mechanical cutting.

2.2 Chip packaging and experiment design

As shown in Fig. 1a, we present our packaged chip with sandwich structure, a PDMS layer about tens of microns in thickness between the glass lid and the wafer acted as an adhesive layer. The thickness of PDMS layer was obtained by cutting off the glass lid with PDMS layer and measuring its cross section by a microscope (IX71, Olympus, Japan). The glass lid is the glass slide commonly used in

micromachining Laboratory; the holes in the glass slide for the inlet and outlets were drilled by laser drilling, and then, a layer of liquid PDMS copolymer was coated on one side by spin coater (KW-4B, Institute of Microelectronics, China). After standing for 12 h, the liquid PDMS layer become hard and smooth. We bonded the side of the glass slide with a layer of PDMS to the wafer by the oxygen plasma cleaner (PDC-001, Harrick, USA); meanwhile, the inlet and outlet positions on the other side were bonded with a thick PDMS for sample injection, respectively, by the same bonding method. At the bottom of the silicon wafer, a 1.99-MHz piezoelectric ceramic (C-213, FUJI Ceramics, Japan) was glued to it by epoxy (Henkel Black& Decker, Germany). A RF signal generator (81150A, Agilent, USA) and a power amplifier (25A250, Amplifier Research, USA) actuated the piezoelectric ceramic at an actual resonance frequency of 2.27 MHz measured by an impedance analyzer, while we monitored the input power by a power meter (PM2003, Amplifier Research, USA). As shown in Fig. 1a, the continuous fluid was introduced into the microfluidic device by syringe pumps (TS2–60, Baoding Longer, China) through poly(tetrafluoroethylene) (PETE) tubes. The collect outlet and waste outlet were at a flow rate of 300 μl/h and 700 μl/h, respectively. Figure 1b shows the sectional diagram orthogonal to the flow channel of the chip packaged by our method. In the figure, the glass slide was packaged to the silicon wafer by the middle PDMS layer, which acted as an adhesive layer to ensure the entire cavity closed without leakage. Ultrasonic standing waves were obtained in the channel of the chip through vibration of the PZT, and the PZT was stuck to the bottom by epoxy. By the sidewalls reflecting the acoustic waves in such channel with a low surface roughness, a standing wave field with a width of a half wavelength was formed in the channel. The particles moved to the pressure nodes in the middle of the channel by acoustic forces.

After finishing the chip fabrication, chip-leaking test was done to check the feasibility of this method. Syringe pump flow speed increased linearly from 100 to 5 ml/h by an increment of 100 μl/h, and no leakage was found during this process. This flow speed was suitable for normal experiment requirement.

3 Results and discussion

3.1 Acoustic theory and numerical simulation of sound pressure

In order to compare with the traditional chip packaged by anodic bonding, we introduce the basic theory of the displacement and force of particles in the channel. The displacement of particle in acoustic standing wave field can be described according to Eq. (1): The displacement(y) which is

Fig. 1 a Schematic diagram of the chip with sandwich structure. Particles can be well enriched in the silicon channel. **b** Cross-section drawing of the assembled separation device along the line ss', the separation channel was sealed with glass slides covered with a PDMS layer and the particles move to the pressure nodes in the middle of the channel
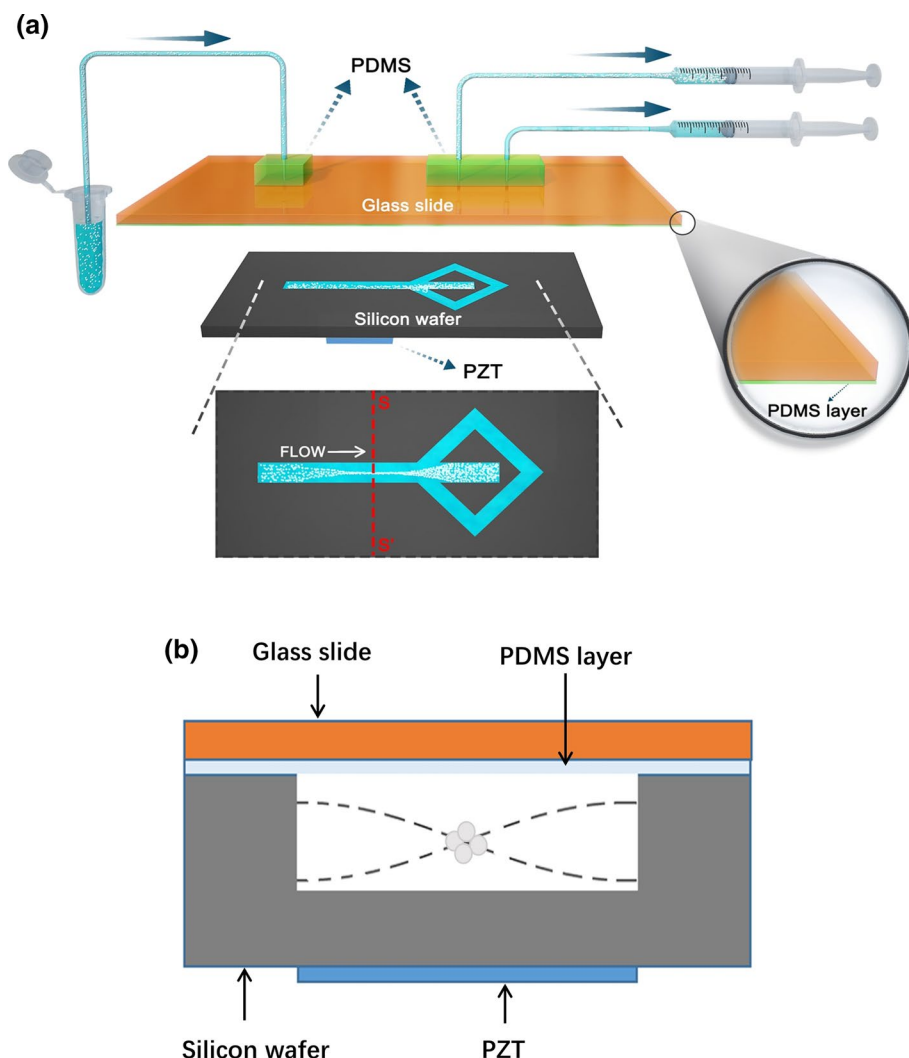
corresponding to a certain position (x) and time (t) is dependent on the amplitude of the standing wave (A) and the wavelength (λ) (Bruus 2012; Shi et al. 2009a).

$$y = A \cos \left(\frac{2\pi x}{\lambda} + \frac{\phi}{2} \right) \sin \left(\frac{2\pi t}{T} + \frac{\phi}{2} \right) \tag{1}$$

When the width of the channel meets half wavelength, the pressure nodes are corresponding to the minimum displacement and at the pressure anti-nodes are corresponding to maximum displacement. The main force acting on a particle can be expressed in the following Eq. (2), in which V_c is the volume of the particle, P_0 is the pressure amplitude and ϕ is defined by Eq. (3). The density of the medium and particles is denoted by two parameters ρ_w and ρ_c, respectively, and the corresponding compressibility is β_w and β_c.

$$F_r = - \left(\frac{\pi P_0^2 V_c \beta_w}{2\lambda} \right) \phi(\beta, \rho) \sin(2kx) \tag{2}$$

$$\phi = \frac{5\rho_c - 2\rho_w}{2\rho_c + \rho_w} - \frac{\beta_c}{\beta_w} \tag{3}$$

When the particle diameter is less than half the wavelength and ϕ is not equal zero, particles move to the middle of the channel and can generally be trapped in the pressure nodes by the acoustic forces. According to these equations, F_r is proportional to V_c, so small particles thus move slower in the medium compared to larger particles.

Laurell's group has done a lot of work based on these theories (Augustsson et al. 2009; Grenvall et al. 2009; Lenshof et al. 2012b). However, the fabrication of traditional acoustic standing waves separation chip is complicated. Anodic bonding for silicon wafer and glass slide is difficult, time-consuming and not safe. Compared to it, our way of chip packaging with sandwich structure is cheap, simple and safe. Besides, our method for chip packaging does cause a certain absorption of acoustic waves and decrease acoustic
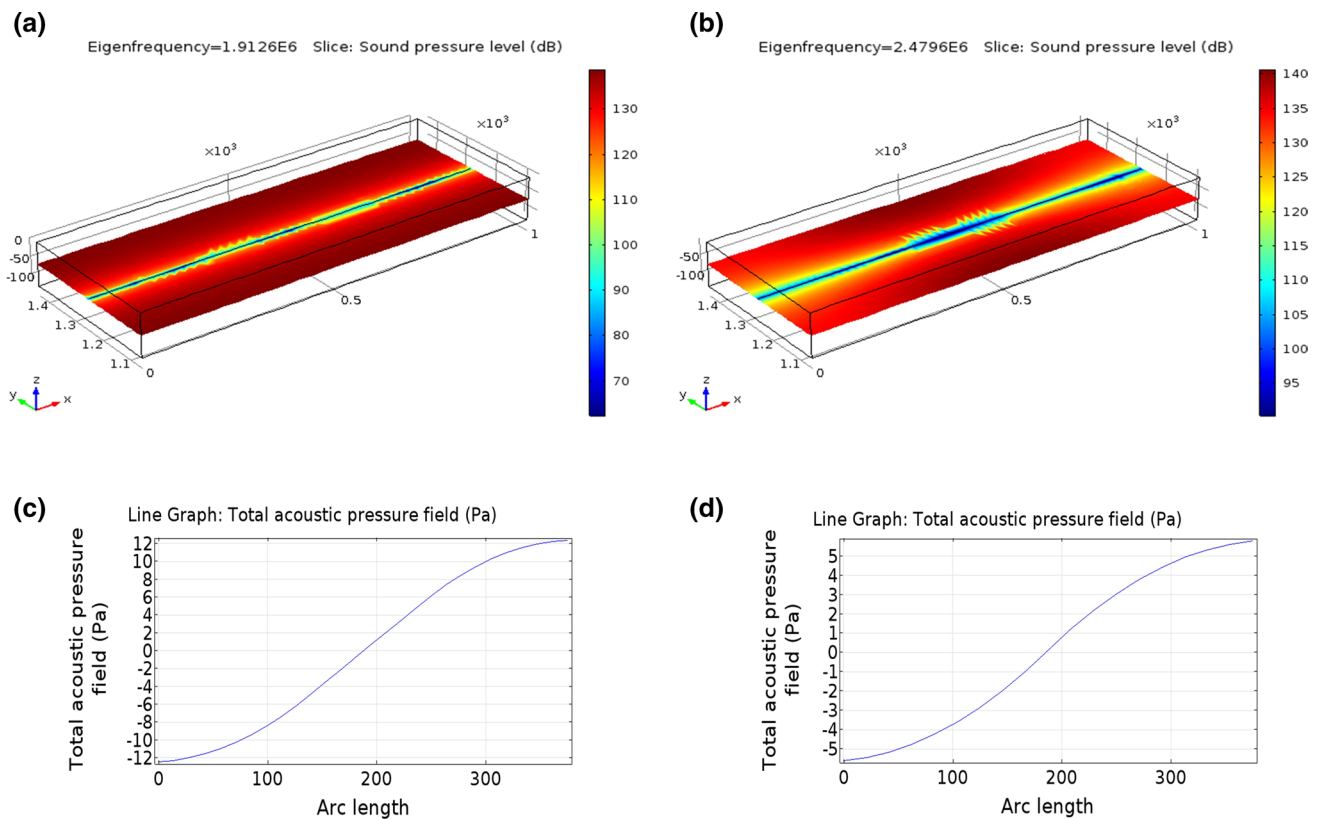
(a)

(b)

(c)

(d)

Fig. 2 **a** The numerical simulation of distribution of sound pressure level in the channel with anodic bonding. **b** The numerical simulation of distribution of sound pressure level in the channel with our packaging method. **c** The numerical simulation of distribution of sound pressure on the cross section of the channel with anodic bonding. **d** The numerical simulation of distribution of sound pressure on the cross section of the channel with our packaging method

forces, but the way to drive particles by acoustic waves is the same with traditional bulk acoustic waves (BAWs) chip when a higher input power is provided.

To study the acoustic absorption of the PDMS layer, we used finite element method in this paper, as shown in Fig. 2. The numerical simulation of distribution of sound pressure level in the channel and sound pressure on the cross section of the channel with anodic bonding is shown in Fig. 2a, c. The numerical simulation of distribution of sound pressure level in the channel and sound pressure on the cross section of the channel with our packaging method is shown in Fig. 2b, d. The all simulation results were conducted by using the finite element method-based software COMSOL Multiphysics. It proves that the influence of PDMS layer on the distribution of acoustic waves in the channel is not large enough. In addition, it can be seen from Fig. 2c, d that the absorption of acoustic waves by the PDMS under 10 V input voltage does decrease by about 50% the acoustic pressure in the channel, but the reduction is acceptable.

3.2 Particle aggregation and optimization of experimental design parameters

Here we characterized our chip performance by experiment of enriching 15-μm silica spheres, and sample was prepared by mixing 0.1-μm silica spheres (Zhiyi Technology Co., China) with 4 ml Triton X-100 (Sigma-Aldrich, Switzerland) solution (0.01%), to avoid aggregation, stirred by a magnetic stirring at a low speed in all the experiment to ensure the particles suspended in the solution. Finally, as shown in Fig. 3, when the PZT (1.99 MHz) was actuated at an actual resonance frequency of 2.27 MHz, the particles were well enriched by acoustic forces.

In order to achieve better enrichment efficiency, we had to optimize the design parameters, which included PDMS design parameters such as the thickness of PDMS layer and the mixing ratio (*A*:*B*) of PDMS layer and input design parameters such as the input power and the sample flow rate. After optimizing these design parameters, we tested the performance of the device and the enrichment efficiency (the number of particles of the collected outlet/the number of particles of the inlet) was greater than 97%.

Fig. 3 Image of 15-μm silica spheres in the BAWs channel with signal off (**a**) and signal on (**b**), the PZT (1.99 MHz) was actuated at an actual resonance frequency of 2.27 MHz
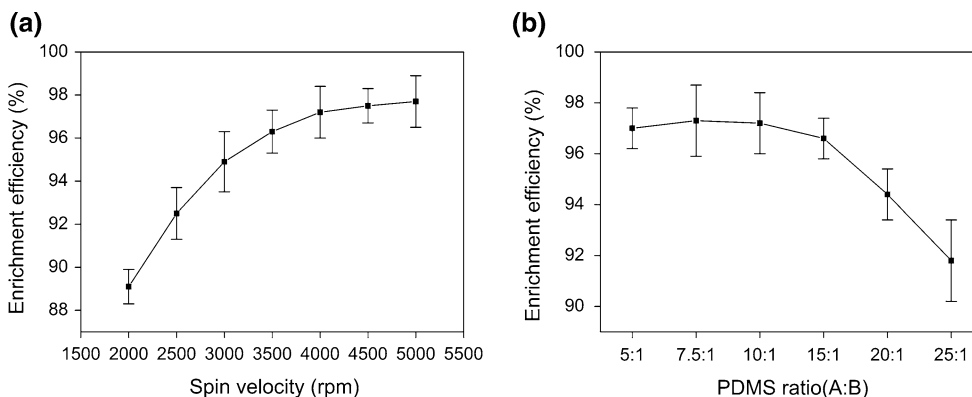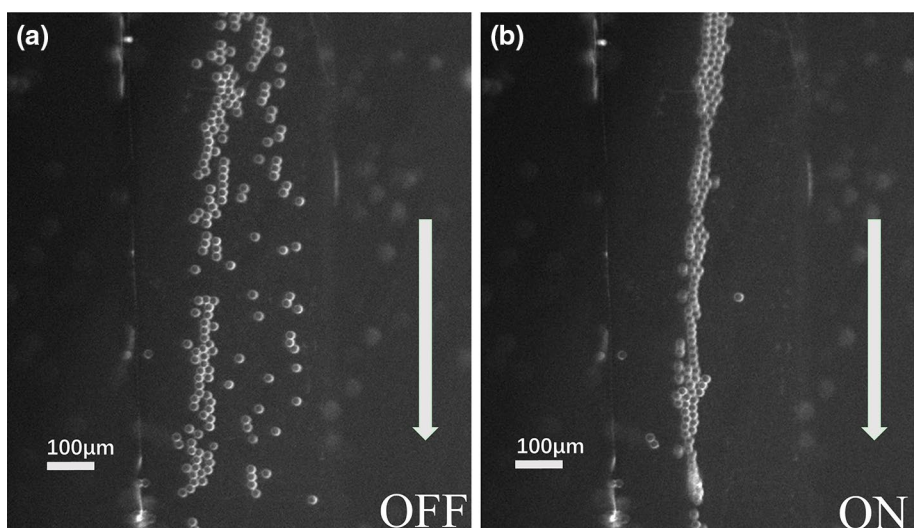

Fig. 4 Enrichment efficiency of chip with sandwich structure as a function of the PDMS design parameters. **a** Enrichment efficiency of chip with sandwich structure as a function of the spin speed. A flow rate of 1 ml/h, input power of 21 dBm and PDMS mixing ratio (*A:B*) of 7.5:1 were used. **b** Enrichment efficiency of chip with sandwich structure as a function of the PDMS mixing ratio (*A:B*). A flow rate of 1 ml/h, input power of 21 dBm and spin speed of 4000 rpm were used

First, we studied the effect of PDMS (*A:B* = 7.5:1) layer thickness on the particle enrichment efficiency. By adjusting the spin speed of spin coater, we got PDMS layer with different thicknesses, and as we originally thought, the thinner the PDMS adhesive layer had a better enrichment efficiency because the thinner PDMS adhesive layer would lead to less acoustic energy attenuation. Figure 4a shows the relationship of enrichment efficiency and spin speed of spin coater. Under the sample flow rate of 1 ml/h and the input power in the 21 dBm, we found that when the spin speed was 4000 rpm corresponding to a thickness of about 35 μm, the enrichment efficiency reached 97.2%. When the speed was more than 4000 rpm, the higher spin speed changed the thickness of PDMS layer little because of the viscosity of PDMS polymer itself, so it led to little increase in particle recovery efficiency. In the latter experiments, we chose

35 μm corresponding to 4000 rpm as the experimental value of the thickness of PDMS layer.

Besides, the mixing ratio (*A:B*) of PDMS also changed the properties of PDMS by influencing the absorption efficiency of acoustic waves in the chip. We studied the relationship between the enrichment efficiency and the PDMS mixing ratio (*A:B*). As expected, the smaller mixing ratio (*A:B*) corresponded to a lower acoustic absorption efficiency. However, the different mixing ratio (*A:B*) of PDMS also affected the thickness in the same spin speed; thus, there should be an optimum PDMS mixing ratio (*A:B*) that could balance these two competing factors. Under a fixed flow rate of 1 ml/h, a input power of 21 dBm and a spin speed of 4000 rpm, we got the relationship between enrichment efficiency and PDMS mixing ratio (*A:B*), as shown in Fig. 4b. In general, the larger mixing ratio (*A:B*) corresponded to a lower enrichment efficiency. When the mixing ratio (*A:B*) was 7.5:1, the
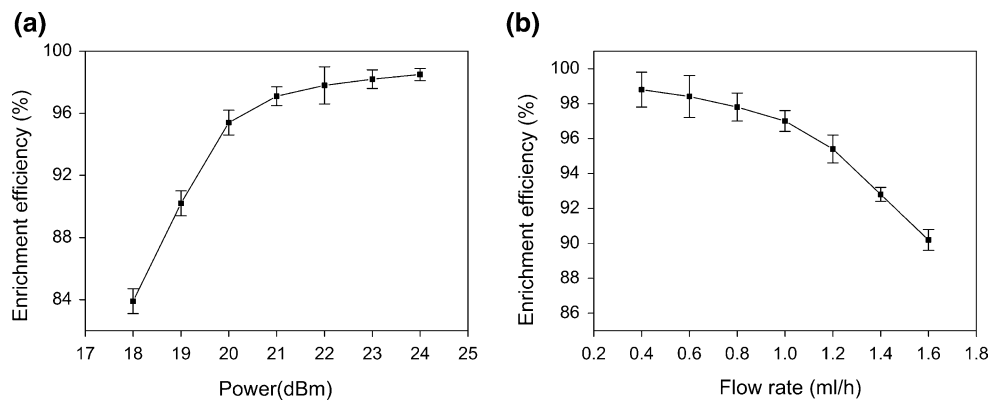
(a)

(b)

Fig. 5 Enrichment efficiency of chip with sandwich structure as a function of the input design parameters. **a** Enrichment efficiency of chip with sandwich structure as a function of the input power to the PZT. A flow rate of 1 ml/h, spin speed of 4000 rpm and PDMS mix-ing ratio (*A*:*B*) of 7.5: 1 were used. **b** Enrichment efficiency of chip with sandwich structure as a function of the flow rate. An input power of 21 dBm, spin speed of 4000 rpm and PDMS mixing ratio (*A*:*B*) of 7.5:1 were used

enrichment efficiency reached maximum value (97.3%). So the PDMS mixing ratio (*A*:*B*) was determined to be 7.5:1 in the latter experiments.

Next, as the PDMS design parameters were fixed, we started to optimize the input design parameters. First, we changed the input power by adjusting the magnification of power amplifier, and the relationship between the enrich-ment efficiency and the input powers was obtained, as shown in Fig. 5a. As expected, the larger power corresponded to higher enrichment efficiency. However, it had no signifi-cant increase when the power efficiency was greater than 21 dBm. Besides, high input power not only caused an increase in temperature in the chip, but also might destroy the piezoelectric properties of the PZT. Therefore, we chose 21 dBm as the optimized input power corresponding to an enrichment efficiency of 97.1%.

At last, by changing the flow rate of the sample under an input power of 21 dBm, spin speed of 4000 rpm and PDMS mixing ratio (*A*:*B*) of 7.5:1, we obtained the relationship between the particle enrichment efficiency and the flow rate of sample. As shown in Fig. 5b, the smaller flow rate of sam-ple corresponded to a higher particle enrichment efficiency, and it was well understood that smaller sample flow rate would make the silica spheres expose to the standing wave field for a longer time, which let more particles move to the pressure nodes in the middle of the channel. When the flow rate was 1 ml/h, we got a high enrichment efficiency of 97%.

4 Conclusions

This paper presents a simple way to package BAWs chip with sandwich structure by using a PDMS layer as an adhe-sive layer, the new BAWs chip can withstand greater pres-sure without leakage, and it can be repeatedly used after

washing. Although a PDMS layer lead to a little acoustic attenuation (Ma et al. 2016; Rambach et al. 2014; Schmid et al. 2011), we could achieve enrichment efficiency of silica spheres for greater than 97% by using low input power, and it proves that our simple packaging method is able to meet the experimental requirements. This work focuses on enrich of silica spheres, but this approach is not limited to it. We demonstrate that the chip with sandwich structure can work well as traditional BAWs chip, so this approach will be also potential in other applications such as blood cleaning, blood component separations and cell sorting (Petersson et al. 2004; Yang and Soh 2012).

References

Antfolk M, Antfolk C, Lilja H, Laurell T, Augustsson P (2015a) A single inlet two-stage acoustophoresis chip enabling tumor cell enrichment from white blood cells. Lab Chip 15:2102–2109. https://doi.org/10.1039/c5lc00078e

Antfolk M, Magnusson C, Augustsson P, Lilja H, Laurell T (2015b) Acoustofluidic, label-free separation and simultaneous concen-tration of rare tumor cells from white blood cells. Anal Chem 87:9322–9328. https://doi.org/10.1021/acs.analchem.5b02023

Augustsson P, Persson J, Ekstrom S, Ohlin M, Laurell T (2009) Decomplexing biofluids using microchip based acoustophoresis. Lab Chip 9:810–818

Bruus H (2012) Acoustofluidics 7: the acoustic radiation force on small particles. Lab Chip 12:1014–1021. https://doi.org/10.1039/c2lc21068a

Ding XY et al (2012) On-chip manipulation of single microparticles, cells, and organisms using surface acoustic waves. Proc Natl Acad Sci USA 109:11105–11109

Dittrich PS, Tachikawa K, Manz A (2006) Micro total analysis systems. Latest advancements and trends. Anal Chem 78:3887–3907

Grenvall C, Augustsson P, Folkenberg JR, Laurell T (2009) Harmonic microchip acoustophoresis: a route to online raw milk sample precondition in protein and lipid content quality control. Anal Chem 81:6195–6200

Grenvall C, Magnusson C, Lilja H, Laurell T (2015) Concurrent isolation of lymphocytes and granulocytes using prefocused free flow acoustophoresis. Anal Chem 87:5596–5604. https://doi.org/10.1021/acs.analchem.5b00370

Guo F et al (2016) Three-dimensional manipulation of single cells using surface acoustic waves. Proc Natl Acad Sci USA 113:1522

Hawkes JJ, Coakley WT, Gröschl M, Benes E, Armstrong S, Tasker PJ, Nowotny H (2002) Single half-wavelength ultrasonic particle filter: predictions of the transfer matrix multilayer resonator model and experimental filtration results. J Acoust Soc Am 111:1259–1266. https://doi.org/10.1121/1.1448341

Hoi SK, Udalagama C, Sow CH, Watt F, Bettiol AA (2009) Microfluidic sorting system based on optical force switching. Appl Phys B-Lasers O 97:859–865

Inglis DW, Riehn R, Austin RH, Sturm JC (2004) Continuous microfluidic immunomagnetic cell separation. Appl Phys Lett 85:5093–5095

Jakobsson O, Oh SS, Antfolk M, Eisenstein M, Laurell T, Soh HT (2015) Thousand-fold volumetric concentration of live cells with a recirculating acoustofluidic device. Anal Chem 87:8497–8502. https://doi.org/10.1021/acs.analchem.5b01944

Lenshof A, Evander M, Laurell T, Nilsson J (2012a) Acoustofluidics 5: building microfluidic acoustic resonators. Lab Chip 12:684–695. https://doi.org/10.1039/c1lc20996e

Lenshof A, Magnusson C, Laurell T (2012b) Acoustofluidics 8: applications of acoustophoresis in continuous flow microsystems. Lab Chip 12:1210–1223. https://doi.org/10.1039/c2lc21256k

Li YL, Dalton C, Crabtree HJ, Nilsson G, Kaler KVIS (2007) Continuous dielectrophoretic cell separation microfluidic device. Lab Chip 7:239–248

Li P et al (2015) Acoustic separation of circulating tumor cells. Proc Natl Acad Sci USA 112:4970–4975. https://doi.org/10.1073/pnas.1504484112

Ma Z, Collins DJ, Ai Y (2016) Detachable acoustofluidic system for particle separation via a traveling surface acoustic wave. Anal Chem 88:5316–5323. https://doi.org/10.1021/acs.analchem.6b00605

Nilsson A, Petersson F, Jonsson H, Laurell T (2004) Acoustic control of suspended particles in micro fluidic chips. Lab Chip 4:131–135. https://doi.org/10.1039/b313493h

Petersson F, Nilsson A, Holm C, Jonsson H, Laurell T (2004) Separation of lipids from blood utilizing ultrasonic standing waves in microfluidic channels. The Analyst 129:938–943. https://doi.org/10.1039/b409139f

Petersson F, Aberg L, Sward-Nilsson AM, Laurell T (2007) Free flow acoustophoresis: microfluidic-based mode of particle and cell separation. Anal Chem 79:5117–5123

Rambach RW, Skowronek V, Franke T (2014) Localization and shaping of surface acoustic waves using PDMS posts: application for particle filtering and washing. RSC Adv 4:60534–60542. https://doi.org/10.1039/c4ra13002b

Ren L et al (2015) A high-throughput acoustic cell sorter. Lab Chip 15:3870–3879. https://doi.org/10.1039/c5lc00706b

Schmid L, Wixforth A, Weitz DA, Franke T (2011) Novel surface acoustic wave (SAW)-driven closed PDMS flow chamber. Microfluid Nanofluid 12:229–235. https://doi.org/10.1007/s10404-011-0867-5

Shi J, Ahmed D, Mao X, Lin SC, Lawit A, Huang TJ (2009a) Acoustic tweezers: patterning cells and microparticles using standing surface acoustic waves (SSAW). Lab Chip 9:2890–2895. https://doi.org/10.1039/b910595f

Shi J, Huang H, Stratton Z, Huang Y, Huang TJ (2009b) Continuous particle separation in a microfluidic channel via standing surface acoustic waves (SSAW). Lab Chip 9:3354–3359. https://doi.org/10.1039/b915113c

Shields CWT, Cruz DF, Ohiri KA, Yellen BB, Lopez GP (2016) Fabrication and operation of acoustofluidic devices supporting bulk acoustic standing waves for sheathless focusing of particles. Journal of Visualized Experiments JoVE. https://doi.org/10.3791/53861

Urbansky A, Lenshof A, Dykes J, Laurell T, Scheding S (2016) Affinity-bead-mediated enrichment of CD8 + lymphocytes from peripheral blood progenitor cell products using acoustophoresis. Micromachines 7:101. https://doi.org/10.3390/mi7060101

Wang MM et al (2005) Microfluidic sorting of mammalian cells by optical force switching. Nat Biotechnol 23:83–87

Yang AH, Soh HT (2012) Acoustophoretic sorting of viable mammalian cells in a microfluidic device. Anal Chem 84:10756–10762. https://doi.org/10.1021/ac3026674

Yu XL et al (2013) Magneto-controllable capture and release of cancer cells by using a micropillar device decorated with graphite oxide-coated magnetic nanoparticles. Small 9:3895–3901